THE EUROPEAN
PHYSICAL JOURNAL C

CrossMark

Stacked search for time shifted high energy neutrinos from gamma ray bursts with the ANTARES neutrino telescope

S. Adrián-Martínez[1], A. Albert[2], M. André[4], M. Anghinolfi[5], G. Anton[6], M. Ardid[1], J.-J. Aubert[3], B. Baret[9,a], J. Barrios-Marti[9], S. Basa[10], V. Bertin[3], S. Biagi[19], R. Bormuth[7,35], M. C. Bouwhuis[7], R. Bruijn[7,28], J. Brunner[3], J. Busto[3], A. Capone[13,14], L. Caramete[15], J. Carr[3], T. Chiarusi[11], M. Circella[18], R. Coniglione[19], H. Costantini[3], P. Coyle[3], A. Creusot[8], I. Dekeyser[20,21], A. Deschamps[17], G. De Bonis[13,14], C. Distefano[19], C. Donzaud[8,22], D. Dornic[3], D. Drouhin[2], A. Dumas[16], T. Eberl[6], D. Elsässer[26], A. Enzenhöfer[6], K. Fehn[6], I. Felis[1], P. Fermani[13,14], F. Folger[6], L. A. Fusco[11,12], S. Galatà[8], P. Gay[16], S. Geißelsöder[6], K. Geyer[6], V. Giordano[31], A. Gleixner[6], R. Gracia-Ruiz[8], K. Graf[6], S. Hallmann[6], H. van Haren[25], A. J. Heijboer[7], Y. Hello[17], J. J. Hernández-Rey[9], J. Hößl[6], J. Hofestädt[6], C. Hugon[5,36], C. W. James[6], M. de Jong[7,35], M. Kadler[26], O. Kalekin[6], U. Katz[6], D. Kießling[6], P. Kooijman[7,27,28], A. Kouchner[8,40], M. Kreter[26], I. Kreykenbohm[29], V. Kulikovskiy[19,30], R. Lahmann[6], D. Lefèvre[20,21], E. Leonora[31,32], S. Loucatos[8,33], M. Marcelin[10], A. Margiotta[11,12], A. Marinelli[23,24], J. A. Martínez-Mora[1], A. Mathieu[3], T. Michael[7], P. Migliozzi[38], A. Moussa[37], C. Müller[26], E. Nezri[10], G. E. Păvălaş[15], C. Pellegrino[11,12], C. Perrina[13,14], P. Piattelli[19], V. Popa[15], T. Pradier[34], C. Racca[2], G. Riccobene[19], R. Richter[6], K. Roensch[6], M. Saldaña[1], D. F. E. Samtleben[7,35], A. Sánchez-Losa[9], M. Sanguineti[36], P. Sapienza[19], J. Schmid[6,b], J. Schnabel[6], F. Schüssler[33], T. Seitz[6], C. Sieger[6], M. Spurio[11,12], J. J. M. Steijger[7], Th. Stolarczyk[33], M. Taiuti[5,36], C. Tamburini[20,21], A. Trovato[19], M. Tselengidou[6], C. Tönnis[9], B. Vallage[33], C. Vallée[3], V. Van Elewyck[8], E. Visser[7], D. Vivolo[38,39], S. Wagner[6], J. Wilms[29], J. D. Zornoza[9], J. Zúñiga[9]

[1] Institut d'Investigació per a la Gestió Integrada de les Zones Costaneres (IGIC), Universitat Politècnica de València, C/ Paranimf 1, 46730 Gandia, Spain
[2] GRPHE-Institut Universitaire de Technologie de Colmar, 34 rue du Grillenbreit, BP 50568, 68008 Colmar, France
[3] CPPM, Aix-Marseille Université, CNRS/IN2P3, Marseille, France
[4] Laboratory of Applied Bioacoustics, Technical University of Catalonia, Rambla Exposició, 08800 Vilanova i la Geltrú, Barcelona, Spain
[5] INFN-Sezione di Genova, Via Dodecaneso 33, 16146 Genoa, Italy
[6] Erlangen Centre for Astroparticle Physics, Friedrich-Alexander-Universität Erlangen-Nürnberg, Erwin-Rommel-Str. 1, 91058 Erlangen, Germany
[7] Nikhef, Science Park, Amsterdam, The Netherlands
[8] APC, Université Paris Diderot, CNRS/IN2P3, CEA/IRFU, Observatoire de Paris, Sorbonne Paris Cité, 75205 Paris, France
[9] IFIC-Instituto de Física Corpuscular, Edificios Investigación de Paterna, CSIC-Universitat de València, c/ Catedrático José Beltrán, 2, 46980 Paterna, Valencia, Spain
[10] LAM-Laboratoire d'Astrophysique de Marseille, Pôle de l' Étoile Site de Château-Gombert, rue Frédéric Joliot-Curie 38, 13388 Marseille Cedex 13, France
[11] INFN-Sezione di Bologna, Viale Berti-Pichat 6/2, 40127 Bologna, Italy
[12] Dipartimento di Fisica dell'Università, Viale Berti Pichat 6/2, 40127 Bologna, Italy
[13] INFN-Sezione di Roma, P.le Aldo Moro 2, 00185 Rome, Italy
[14] Dipartimento di Fisica dell'Università La Sapienza, P.le Aldo Moro 2, 00185 Rome, Italy
[15] Institute for Space Sciences, 77125 Bucharest, Măgurele, Romania
[16] Laboratoire de Physique Corpusculaire, Clermont Université, Université Blaise Pascal, CNRS/IN2P3, BP 10448, 63000 Clermont-Ferrand, France
[17] Géoazur, Université Nice Sophia-Antipolis, CNRS/INSU, IRD, Observatoire de la Côte d'Azur, Sophia Antipolis, France
[18] INFN-Sezione di Bari, Via E. Orabona 4, 70126 Bari, Italy
[19] INFN-Laboratori Nazionali del Sud (LNS), Via S. Sofia 62, 95123 Catania, Italy
[20] Mediterranean Institute of Oceanography (MIO), Aix-Marseille University, 13288 Marseille Cedex 9, France
[21] Université du Sud Toulon-Var, CNRS-INSU/IRD UM 110, 83957 La Garde Cedex, France
[22] Université Paris-Sud, 91405 Orsay Cedex, France
[23] INFN-Sezione di Pisa, Largo B. Pontecorvo 3, 56127 Pisa, Italy
[24] Dipartimento di Fisica dell'Università, Largo B. Pontecorvo 3, 56127 Pisa, Italy
[25] Royal Netherlands Institute for Sea Research (NIOZ), Landsdiep 4, 1797 SZ 't Horntje, Texel, The Netherlands
[26] Institut für Theoretische Physik und Astrophysik, Universität Würzburg, Am Hubland, 97074 Würzburg, Germany
[27] Faculteit Betawetenschappen, Universiteit Utrecht, Princetonplein 5, 3584 CC Utrecht, The Netherlands
[28] Instituut voor Hoge-Energie Fysica, Universiteit van Amsterdam, Science Park 105, 1098 XG Amsterdam, The Netherlands
[29] Dr. Remeis-Sternwarte and ECAP, Universität Erlangen-Nürnberg, Sternwartstr. 7, 96049 Bamberg, Germany

[30] Skobeltsyn Institute of Nuclear Physics, Moscow State University, Leninskie gory, 119991 Moscow, Russia

[31] INFN-Sezione di Catania, Viale Andrea Doria 6, 95125 Catania, Italy

[32] Dipartimento di Fisica ed Astronomia dell'Università, Viale Andrea Doria 6, 95125 Catania, Italy

[33] Direction des Sciences de la Matière, Institut de recherche sur les lois fondamentales de l'Univers, Service de Physique des Particules, CEA Saclay, 91191 Gif-sur-Yvette Cedex, France

[34] IPHC-Institut Pluridisciplinaire Hubert Curien, Université de Strasbourg et CNRS/IN2P3, 23 rue du Loess, BP 28, 67037 Strasbourg Cedex 2, France

[35] Leids Instituut voor Onderzoek in Natuurkunde, Universiteit Leiden, 2333 CA Leiden, The Netherlands

[36] Dipartimento di Fisica dell'Università, Via Dodecaneso 33, 16146 Genoa, Italy

[37] Laboratory of Physics of Matter and Radiations, University Mohammed I, B.P.717, 6000 Oujda, Morocco

[38] INFN-Sezione di Napoli, Via Cintia, 80126 Naples, Italy

[39] Dipartimento di Fisica dell'Università Federico II di Napoli, Via Cintia, 80126 Naples, Italy

[40] Institut Universitaire de France, 75005 Paris, France

Abstract A search for high-energy neutrino emission correlated with gamma-ray bursts outside the electromagnetic prompt-emission time window is presented. Using a stacking approach of the time delays between reported gamma-ray burst alerts and spatially coincident muon-neutrino signatures, data from the ANTARES neutrino telescope recorded between 2007 and 2012 are analysed. One year of public data from the ICECUBE detector between 2008 and 2009 have been also investigated. The respective timing profiles are scanned for statistically significant accumulations within 40 days of the Gamma Ray Burst, as expected from Lorentz Invariance Violation effects and some astrophysical models. No significant excess over the expected accidental coincidence rate could be found in either of the two data sets. The average strength of the neutrino signal is found to be fainter than one detectable neutrino signal per hundred gamma-ray bursts in the ANTARES data at 90% confidence level.

1 Introduction

Gamma-ray bursts (GRBs) are among the most powerful sources in the universe, which makes them suitable candidates for the acceleration of the highest-energy cosmic rays. Unambiguous evidence for the acceleration of hadrons in astrophysical environments can be provided by the detection of neutrinos that would be coincidently produced when accelerated protons interact with the ambient photon field (see, e.g. [1–3] and references therein). Searches for the emission of neutrinos from GRBs have been performed by a variety of experiments, for instance Super-Kamiokande [4], AMANDA [5], Baikal [6], RICE [7], ANITA [8], IceCube [9,10] and ANTARES [11,12]. While covering a wide range of neutrino energies these studies have so far focussed mainly on the time window coincident with the electromagnetic signal of GRBs. Up to now no neutrino signal could be identified by any neutrino detector during the prompt emission phases, and analytical models from [13] based on [2] have already been excluded by the IceCube collaboration [10]. There has also been some effort to successively extend the search time windows in the IceCube data from [−1 h, +3 h] up to ±1 day [9,10], and up to ±15 days [14], to account for prolonged neutrino emission. However none of these searches could bring compelling evidence for a GRB signal, since all detected events have been identified with cosmic-ray induced air showers or were of low significance because of the large time windows.

While the search for a signal of neutrinos coincident with the emission of high-energy photons is the most common ansatz, there are many models that predict time-shifted neutrino signals, such as neutrino precursors [15], afterglows (e.g. [16]), or different Lorentz Invariance Violation (LIV) effects for photons and neutrinos on their way to Earth [17,18]. For instance, the possibility that three low significance neutrino-like events found in the IceCube data [10] could have been produced by GRBs but arrived before the photon signal due to LIV effects is discussed in [19]. Probing such scenarios requires a new approach to the search for correlated emission. Moreover, in all aforementioned scenarios, the neutrino signal is simply shifted in time with respect to the electromagnetic signal, and none of these models predict any considerably prolonged neutrino emission. Hence the approach used in this paper and described in Sect. 3 aims at identifying a presumably faint neutrino signal that is shifted with respect to the electromagnetic GRB emission by an unknown time offset, while making no assumption about the origin of such an offset.

[a] e-mail: baret@in2p3.fr

[b] e-mail: Julia.schmid@fau.de

2 Neutrino candidates and GRB sample

Neutrino telescopes are arrays of photomultipliers deployed in a very large volume of transparent medium like Antarctic ice or deep-sea water. They detect the Cherenkov light generated by the products of the interaction of a high-energy neutrino in the vicinity of the detector. The direction of the impinging neutrino is reconstructed using the timing of signals from photomultipliers, while the detected amount of light gives an estimate of the neutrino energy. The ANTARES telescope [20] is located at a depth of 2475 m in the French Mediterranean Sea off the coast of Toulon, at 42°48′N, 6°10′E. It comprises 885 optical modules housing 10″ photomultipliers in 17″ glass spheres installed on 12 strings, representing an instrumented volume of 0.02 km^3.

The following analysis focuses on the detection of muon trajectories from below the horizon, which are produced by muon-neutrino charged-current interactions. This channel provides significantly better directional reconstruction than neutral-current interactions and charged current interactions from the other neutrino flavors. In this channel, ANTARES is the most sensitive detector for sources in a large part of the southern sky up to a few 100 TeV [21].

The sample of ANTARES events used in this analysis consists of 5516 neutrino candidates selected from data collected between March 2007 and the end of 2012 [22]. From Monte Carlo simulations the angular resolution, defined as the median of the space angle δ_{err} between the true and reconstructed direction of neutrinos for an E^{-2} differential spectrum, is 0.38°, with a contamination from atmospheric muons of 10%. The right-ascension distribution of the neutrino candidates is shown in Fig. 1.

A suitable GRB sample was consolidated similarly to the one used in [12]. It was built using catalogs from the *Swift* [23] and *Fermi* satellites [24,25], and supplemented by a table from the ICECUBE Collaboration[1] [26], with information parsed from the GRB Coordinates Network (GCN) notices. Since only the time and position information (and the measured redshift, if available) of each announced GRB was used, no further selection on e.g. the quality of the spectral measurements was required, leading to 1488 GRBs. Only GRB alerts were taken into account that occurred both below the horizon of the neutrino telescope and during the covered neutrino data collection period. The upper panel of Fig. 2 shows the distribution of the selected neutrino candidates, which are homogeneously distributed in time. The lower panel displays the accordingly selected GRBs in equatorial coordinates and their measured fluence.
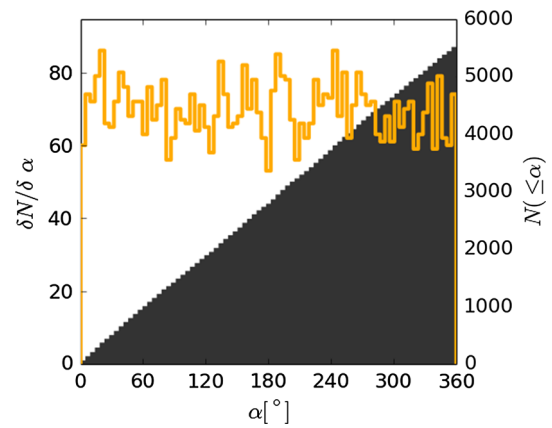
Fig. 1 Distribution of the right ascension α of the ANTARES neutrino event sample (March 2007–December 2012). The respective cumulative distribution is shown in *black*
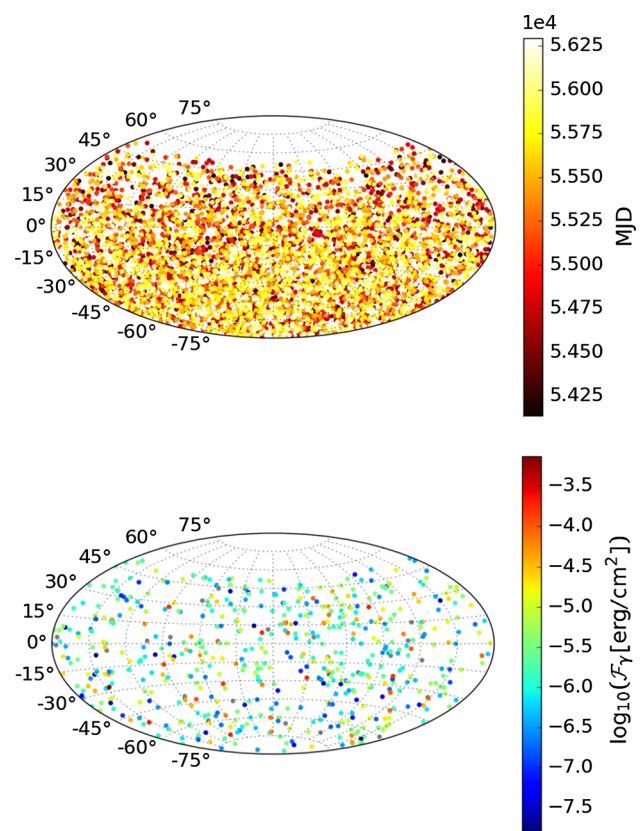

Fig. 2 Distributions in equatorial coordinates of selected GRBs (*upper panel*) and recorded neutrino candidates (*lower panel*) for the ANTARES event sample. Each GRB's location is color-coded with the photon fluence $\mathcal{F}_\gamma$; those with no measurement are coloured in *gray*. The *color* of neutrino events represents their detection time

3 Principle of the search

Neutrino signatures are searched-for in an angular cone around the direction of, and within a maximum time offset from the time of each GRB. For any such space and time

coincidence, the time difference with respect to the GRB alert is recorded. In order to avoid any boundary effect such as an artificial asymmetry of neutrino candidates around a GRB alert close to the beginning or end of neutrino telescope data taking, GRBs detected during a period of half the considered maximum time offset at the beginning and end of the neutrino data sample are excluded. The collected time differences are stacked in a common timing profile. In the case of no signal, only purely accidental spatial coincidences of the neutrino candidates with the defined search cones around the GRB positions would be expected. The observed time shifts should then be distributed randomly, yielding a flat stacked distribution where all shifts are equally likely. Any neutrino emission associated with the GRBs, even if faint, can give rise to a cumulative effect in these stacked profiles, which can then be identified by its discrepancy from the background hypothesis. An optimal choice of the search cone size δ_{max} naturally depends on the GRB's position accuracy and the neutrino direction reconstruction uncertainty. The size of the probed time window τ_{max} should be defined as the largest shift predicted by any of the models under consideration. Such a procedure had already been proposed [27], where windows of ± 1 h around the GRB satellite triggers under study were considered. The approach presented in the following is extended to allow significantly larger time windows and different origins of the time shift. This method is intrinsically different from those previously developed by the ICECUBE Collaboration [10,14], which focused on successively widening symmetric search time windows around the GRB alerts considering a flat temporal signal probability density function. In the case of a time-shifted signal, these methods suffer from reduced significance due to the accumulated background in the increasingly large time windows. In contrast, the technique presented here aims at identifying a time-shifted signal as a peak on top of flat background.

3.1 Potential physical delays considered

For maximum generality we perform a test for a constant offset ($\tau = t_\nu - t_{GRB}$) between the (first) detected photon signal t_{GRB} and the time of a possibly associated neutrino candidate t_ν, for maximum generality. In the case of a constant shift τ_{em} of the emission times of the neutrino with respect to photons at the source, it translates into observed time delays at Earth τ_{obs} that depend on the cosmological redshift z of the GRB as:

$$\tau_{em} = \tau_{obs}/(1+z). \tag{1}$$

To test for these intrinsic time shifts, the distribution of $\tau_z = \tau/(1+z)$ will be investigated. Note that the redshift is only measured for approximately 10% of all GRBs, significantly reducing the statistics of the stacked profile when omitting all GRBs without determined redshift.

Effects due to LIV (see e.g. [17–19]) can also yield different arrival times at Earth for photons and neutrinos of high energy produced by a GRB. In a variety of quantum spacetime models, the velocity dispersion relation linking the energy of the particle E and its momentum p is modified by an additional term proportional to an integer power of the ratio of the energy to the Planck scale:

$$E^2 - p^2 c^2 = \pm E^2 \cdot (E/M_{LIV})^n, \tag{2}$$

where M_{LIV} is the scale at which the symmetry is broken. The mass term $m^2 c^4$ can be neglected for neutrinos [18]. First-order terms with $n = 1$ will be considered here as these exhibit the most sizeable effects. Within this framework, the time shift observed at Earth will depend on the energy of the neutrino, the distance of the source $D(z)$ and the energy scale M_{LIV}:

$$\Delta t_{LIV} = (\pm 1) \cdot E/M_{LIV} \cdot D(z)/c, \tag{3}$$

where $D(z)$ is the effective distance travelled by the particles taking into account the expansion of the Universe, and is defined according to [19] as:

$$D(z) = \frac{c}{H_0} \int_0^z \frac{(1+z')dz'}{\sqrt{\Omega_m(1+z')^3 + \Omega_\Lambda}}, \tag{4}$$

where z is the redshift, H_0 is the Hubble constant, and Ω_m and Ω_Λ are the relative matter and dark energy densities of the Universe [29]. These effects are expected to appear in a stacked histogram that accounts for both the estimated neutrino energy E_{est} and the distance of the source. Consequently, the variable to be probed is defined as:

$$\tau_{LIV} = \frac{\tau}{E_{est} \cdot D(z)}, \tag{5}$$

In case of a sizeable LIV effect, with a given value of M_{LIV} this yields

$$\tau_{LIV} \propto \pm \frac{E}{E_{est}} \cdot \frac{1}{M_{LIV} \cdot c}, \tag{6}$$

and the time-stacked neutrino observations will accumulate around a single value of τ_{LIV}. In contrast, the distribution of events due to purely accidental coincidences will peak around zero.

The ratio $r = n_+/n_-$ of spatially coincident events before and after the respective GRB alert is a very simple measure to probe the distributions while making the fewest assumptions on any model. Any effect leading to different arrival times of neutrinos and gamma-rays from GRBs is expected to yield either positive or negative time shifts. This ratio is calculated if both n_+ and n_- are non-zero.

Consequently, in the search for an associated neutrino signal from GRBs, three stacked time profiles for the measures τ, τ_z and τ_{LIV} were generated for all neutrino candidates

which matched the coordinates of a reported GRB alert, and the ratio r for the whole sample was computed.

4 Implementation of the method and application to ANTARES 2007–2012 data

The expected number of background events μ_b increases with the solid angle of the search cones $\Omega(\delta_{\max})$ around each GRB's position and with the considered maximum time delay $\tau_{\max}$. Hence, the choice of the search cone size and the probed time window should be optimised under reasonable physical considerations.

4.1 Search cone

The determination of an optimally-sized search cone for spatially coincident neutrino candidates with a GRB alert was based on the maximisation of the ratio of signal to square root of background. Assuming a point-source-like signal at the GRB's location, the reconstructed neutrino directions approximately follow a two-dimensional Gaussian profile of standard deviation σ_ν around this position. This approach yields an optimum search cone size of $1.58 \cdot \sigma_\nu$ as derived for example in [30]. Note that the neutrino telescope resolution is usually stated as the median of the reconstructed direction error $m(\delta_{\mathrm{err}})$ (see for instance [31]). For angles in consideration here, the relation $m(\delta_{\mathrm{err}}) \sim 1.17\sigma_\nu$ holds.

The effects of uncertainty in GRB location Δ_{err} (sub-arc second for *Swift*/UVOT or ground based telescopes, up to several degrees for *Fermi*/GBM) is accounted for by extending the search window whenever $\Delta_{\mathrm{err}} > \sigma_\nu$. As the contribution of random coincidences scales quadratically with Δ_{err}, the background in the cumulative profile might be dominated considerably by a few bursts with very large satellite error boxes. Consequently, a reasonable trade-off should be found. On the one hand, the statistics should not be reduced too much by excluding a large number of badly-localised bursts. On the other hand, the stacked timing profiles should not be dominated by one burst with a large error box, which naturally leads to many accidental spatial coincidences. In order to limit this effect without significantly reducing the data sample, a maximum search-cone size was chosen – based on the distribution of $\Delta_{\mathrm{err}}^{\max}$ shown in Fig. 3 – such that no GRB contributed more than an order of magnitude more of uncorrelated background than any other.

The search-cone size is consequently defined as:

$$\delta_{\mathrm{cut}} = 1.58 \cdot \max(\sigma_\nu, \, \min(\Delta_{\mathrm{err}}, \Delta_{\mathrm{err}}^{\max})). \tag{7}$$

Using the ANTARES pointing resolution of $0.38°$, all bursts with error boxes larger than $\Delta_{\mathrm{err}}^{\max} = 1°$ were consequently discarded from the search, which reduced the sample by $\sim54\%$ while keeping 74% of the total gamma-ray flu-
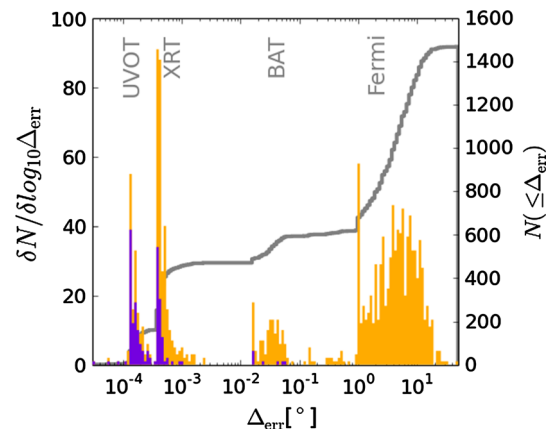

Fig. 3 Number of GRBs with a given error box Δ_{err} (*orange*). The cumulative distribution is shown by the *grey line*. For GRBs with measured redshift, the distribution is shown in *violet*

ence of the sample, yielding search-cone sizes in the range $[0.51°, 1.58°]$. Note that Fermi-detected bursts with a resolution of $1°$ are included.

4.2 Maximum time delay

The approach presented in this paper aims at being as model independent as possible. The maximum time shift anticipated from the astrophysical processes mentioned in Sect. 3.1 is used to set the time coincidence window. Intrinsic shifts in the emission times of neutrinos were predicted in [15] with neutrinos ~100 s before the electromagnetic GRB signal. A precursor neutrino signal that might be emitted even tens of years before the actual GRB is derived in [32]. Since the latter time scale exceeds the operational times of the current neutrino telescopes, we will omit this scenario. Early afterglow emission of neutrinos ~10 s after the burst are predicted in [16,33] and extended neutrino fluxes up to 1 day after the prompt emission are derived in [34]. These intrinsic time shifts between neutrino and photon signals are still well within the time scopes that have already been probed, for example in [10,14] – without positive result.

Differences in arrival times induced by LIV effects would depend not only on M_{LIV}, but also on the energy of the particles and the distance of the source. However, a maximum expected time shift of neutrinos and photons can be inferred from Eq. 3 using the existing limit on the LIV energy scale. The most stringent limit within the theoretical framework used here has been set to $M_{\mathrm{LIV}} = 7.6 \cdot M_{\mathrm{Planck}}$ based on the *Fermi*/LAT data [35]. Using the distance $D(z)$ at a redshift of $z = 8.5$, which is the highest measured redshift in the selected GRB catalog, and a maximum energy of $\sim E_{\max} = 10^9$ GeV accounting for the energy range at which a signal might be observed, a maximum time shift of $\tau_{\max} = 40$ days was derived. Even though the upper bound was derived from

quantum space-time models, the search itself remains model independent.

A discretisation of the cumulative timing profiles into 150 bins was chosen, which allows time scales down to 13 h to be probed. Given the low number of expected coincidences within the allowed time window (see Sect. 4.5), this choice ensures that there will be much less coincidences than bins, leading to a quasi-unbinned approach [28].

4.3 Final GRB sample

Having chosen the maximal search time window and the largest angular search cone that should be taken into account, the final samples associated with the neutrino telescope data set were determined. The initially selected GRB catalog comprised 1488 bursts that had occurred between 2007 to 2012, which gives a detection rate of 0.68 bursts per day. Out of these, 563 have been selected for the search of associated neutrinos in the ANTARES data using the criteria outlined above, of which 150 have a measured redshift z.

4.4 Statistical tests

From the stacked histograms of τ, τ_z and τ_{LIV}, test statistics are calculated that distinguish a systematically time-shifted neutrino signal associated with GRBs from the background-only hypothesis of purely accidental coincidences. A large number of background realisations preserving the telescope's acceptance are generated from the existing data sets by scrambling the time from the corresponding distribution of Fig. 1 and randomising the right ascension of detected neutrino candidate events in accordance with the flatness of the data distribution. The significance, of an excess in the data is then given by the p-value which is the probability to measure the test statistic in question (or more extreme values) from the background-only distribution.

The test statistic associated to the ratio r will be the variable itself. For the stacked histograms, the Bayesian observable ψ to estimate the compatibility of a given stacked (and binned) time profile with the expectations from background has been proposed in [27,28]. This test statistic is proportional to the logarithm of the probability p of an observation D under an hypothesis H defined by a set of information I (here that the stacked profile bins are filled following a multinomial law of known probabilities):

$$\psi = -10 \log_{10} p(D|H, I)$$
$$= -10 \left[\log_{10} n! + \sum_{k=1}^{m} n_k \log_{10} p_k - \log_{10} n_k! \right], \quad (8)$$

with n events in the histogram in total, distributed in $k \in [1 \ldots m]$ bins. The probability to fall within bin k is p_k; for a uniform background distribution (i.e. in the case of the

τ profile), $p_k = 1/m$ is simply given by the total number of bins m. For the non-uniform profiles τ_z and τ_{LIV}, these probabilities have to be determined by a large number of pseudo-experiments simulating the background, of the order of 10^7 to estimate the significance of a potential excess up to the 5σ level. The value of ψ is calculated for each of the τ, τ_z and τ_{LIV} profiles, correspondingly denoted ψ, ψ_z and ψ_{LIV}.

4.5 Sensitivity

Around 1.4×10^7 pseudo experiments yielding sky-maps of uncorrelated neutrino events were generated to simulate the case of purely accidental coincidences (background-only) between the ANTARES neutrino data and the GRB catalogue. On average, 3.9 of the neutrino candidates are expected to match the bursts' search windows in time and space, with 0.7 of them coinciding accidentally with the bursts with measured redshift.

To illustrate the performance of the proposed technique to identify hypothetical neutrinos from GRBs, a test signal was generated by associating neutrino candidates artificially with a fraction of the GRBs at a hypothetical intrinsic time shift of t_{in} with $t_{in} = 1, 5, 10$ or 20 days. That is, taking into account the cosmological redshift z, a simulated signal delayed by $t_\nu = t_{GRB} + t_{in} \cdot (1+z)$. Its strength was quantified by the probability $f \in [0, 1]$ that a GRB produced a signal in the neutrino telescope. The signal was consequently only simulated for those bursts for which the redshift could be determined, and the variable which has the best sensitivity to it will be τ_z since signal will accumulate in one bin.

The discovery probability $\mathcal{MDP}$ at $n\sigma$ significance level for a given signal strength is given by the fraction of realisations that lead to values of the test statistics (here r, ψ, ψ_z or ψ_{LIV}) above a threshold corresponding to a p-value at the $n\sigma$ level on the background-only realisations. It represents the efficiency of the analysis and the specific test statistic to identify a signal being associated with a fraction of GRBs. The detection efficiency of the ψ_z test statistic is independent of the time shift of signal for delays up to 10 days, as can be seen in Fig. 4. The evolution of the efficiencies for an example signal at an intrinsic time shift of 5 days as a function of the signal strength f is shown in Fig. 5, and is hence representative of shifts from 0 to 10 days. Signal strength corresponding to discovery probabilities are summarized in Table 1, for the whole sample and for GRBs with measured redshift. For instance, using the ψ test statistics, if only $f = 1.3\%$ of the GRBs would give rise to an associated signal neutrino, it would produce an excess of 3σ significance with 50% probability, whereas a stronger signal in 2.4% of the bursts would be identified at the 5σ level. For the sample of GRBs with measured redshift, the ψ_z test statistic only needs a fraction $f_z = 4.5\%$ which is half of the signal fraction necessary with the ψ test statistic for the same detection efficiency.
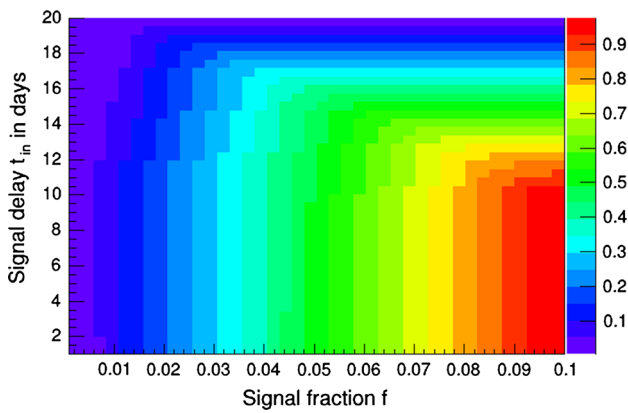
Fig. 4 Detection efficiency (*color scale*) at the 3σ level using the ψ_z test statistic as a function of the signal strength f (see text) and intrinsic time delay at the source for a signal as described in Sect. 4.5
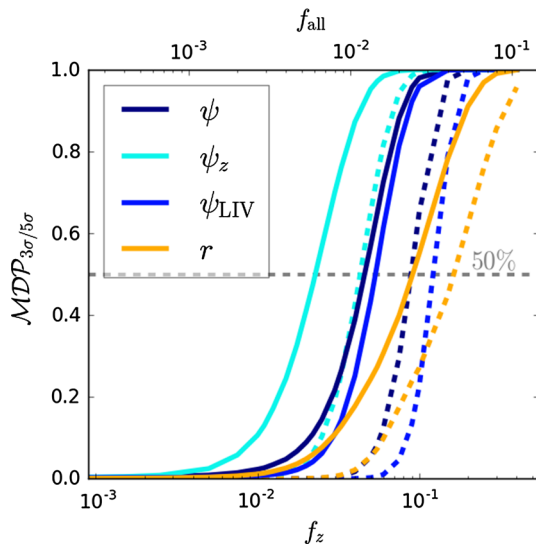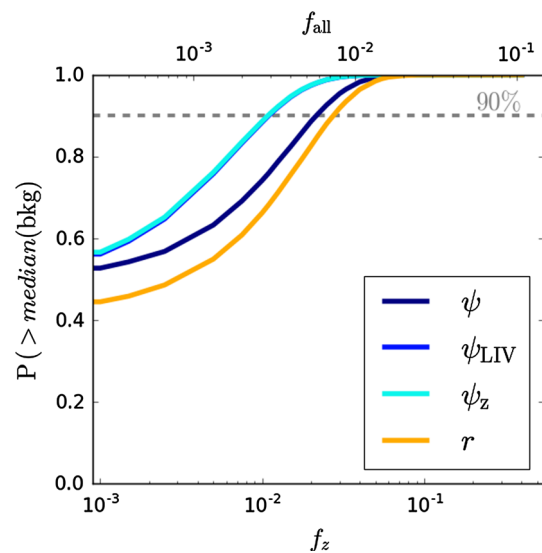

Fig. 6 Probabilities P to measure values of the test statistics above the median value from the background-only realisations as a function of f_z or f_{all} (as in Fig. 5). The sensitivity is given by the signal fraction f where the curves reach 90% probability (*grey dashed line*). Note that the curves for ψ_z and ψ_{LIV} lie on top of each other. Probabilities were derived using the ANTARES data from 2007–2012

Fig. 5 Detection probability $\mathcal{MDP}$ at 3σ (*solid*) and 5σ (*dashed lines*) for the test statistics ψ, ψ_z, ψ_{LIV} and r as a function of the mean fraction f of GRBs with one associated signal neutrino at $t_\nu = t_{GRB} + 5d \cdot (1 + z)$. The fraction f_z denotes the fraction of GRBs in the sample with determined redshift z, whereas f_{all} gives the fraction of the whole sample

The introduced time-stacking technique is consequently capable of robustly finding at the 3σ level an intrinsically delayed neutrino emission from GRBs as long as it is associated with at least 3 of the 563 bursts.

The probability of measuring values of the test statistics exceeding the median background value for different signal strengths is shown in Fig. 6. The sensitivity at 90% (99%) confidence-level (CL) is defined as the 90% (99%) CL upper limit that can be placed on the signal strength when observing the median background (see gray dashed line marking 90%). The sensitivities at 90% and 99% CL of the proposed analysis for the given test signal simulating neutrino emission delayed by five days at the source in a mean fraction of all bursts are summarised in Table 1. For instance, at 90% CL, considering only the sub-sample of bursts with determined redshift and the test statistics ψ_z and ψ_{LIV}, the method is sensitive to a signal in only 1.1% of the bursts (Table 1).

Table 1 Sensitivities at 90% and 99% confidence level and detection probabilities at 3σ and 5σ with 50% statistical power for a signal delayed by 5 days at the source (see text) for the different test statistics expressed in terms of the fraction f_{all} of the GRB sample with detectable signal and the fraction f_z of the GRB sample with measured redshift f_z

Test statistic	Sensitivity at 90% CL		Sensitivity at 99% CL		$\mathcal{MDP}$ 3σ		$\mathcal{MDP}$ 5σ	
	f_{all} (%)	f_z (%)	f_{all} (%)	f_z (%)	f_{all} (%)	f_z (%)	f_{all} (%)	f_z (%)
r	0.8	3.0	1.5	5.5	2.4	9.0	4.5	17
ψ	0.6	2.2	1.3	5.0	1.3	5.0	2.4	9.0
ψ_z	0.3	1.1	0.8	3.0	0.6	2.3	1.2	4.5
ψ_{LIV}	0.3	1.1	0.8	3.0	1.5	5.5	3.0	12.5

Table 2 Probabilities P to yield values of the test statistic $Q \in [\psi, \psi_z, \psi_{LIV}]$ above the measurement Q_{meas} and above the median value $m(Q)$ as expected from pure background realisations for differ-
ent fractions f_{all} (f_z) of all GRBs (with measured redshift z) with one associated signal neutrino intrinsically shifter by 5 days at the source

f_{all} (%)	$P(>\psi_{meas})$ $\psi_{meas} = 0$ (%)	$P(>m(\psi))$ $m(\psi) = 73.3$ (%)	f_z (all z) (%)	$P(>\psi_{z,meas})$ $\psi_{z,meas} = 0$ (%)	$P(>m(\psi_z))$ $m(\psi_z) = 0$ (%)	$P(>\psi_{LIV,meas})$ $\psi_{LIV,meas} = 0$ (%)	$P(>m(\psi_{LIV}))$ $m(\psi_{LIV}) = 0$ (%)
0.0	98	50	0.0	48.5	48.5	48.2	48.2
0.04	99	54	0.15	59	59	59	59
0.29	99	75	1.1	90	90	90	90
0.60	100	90	2.3	98	98	98	98
0.69	100	93	2.6	99	99	99	99
1.07	100	98	4.0	100	100	100	100
1.33	100	99	5.0	100	100	100	100
2.10	100	100	8.0	100	100	100	100

5 Results and discussion

The data collected by the ANTARES telescope from the years 2007 to 2012 were analysed to search for neutrinos within the predefined angular and timing search windows associated with the GRB catalogue. None of the neutrino candidates in the data matched these search windows, where 3.9 would have been expected from background (0.7 coincidences were expected for the GRBs with measured redshift z). The measured values of the test statistics are thus zero, and the ratio $r = n_+/n_-$ is undefined. The probability to observe no events coinciding with all GRBs is relatively small, with $P(0|3.9) = 1.2\%$ (and 51.4% for GRBs with measured z).

We verified the under-fluctuation to be of statistical origin instead of intrinsic systematic effects in the search methodology or the software. In particular, we derived the number of coincidences when increasing independently τ_{max} and δ_{max}. Using these enlarged coincidence windows, the number of coincident data events is close to the expected number of coincidences from randomized data.

In Table 2, the probabilities P to measure test statistics above the measurements and the expected values from the median background realisations are given. This results in 99% CL limits of $f_{all} = 0.04\%$ and $f_z = 2.6\%$, and a 90% CL upper limit on f_z of 1.1%. With the aforementioned under-fluctuation, the setting of a 90% CL limit on f_{all} defined according to Sect. 4.5 is not possible. A conservative option would be to set the limit equal to the sensitivity as in [36]. Since this method does not make use of the information contained in the actual nonobservation, the resulting 90% CL of $f_{all} = 0.6\%$ is weaker than the standard 99% CL of 0.04%, so the value of 0.04% should be used for both 90% and 99% CL.

We can state a sensitivity of $m(f_{all}^{90\%CL}) = 0.6\%$ of all GRBs (2.2% for those with measured z), which is the median upper limit on the fraction of bursts that contain a signal of

the form $\tau_s = 5\,\text{d} \cdot (1+z)$. Furthermore, we see that 99% of all realisations with a signal fraction $f_{all} = 0.04\%$ would yield higher ψ than observed, so we can exclude such a signal with 99% confidence. Regarding the sample of bursts with measured redshift z, the observation of zero events matched the median expectation from background, so we could exclude that 1.1% of them produced a signal neutrino with a delay shape $\tau_s = 5\,\text{d} \cdot (1+z)$ with 90% confidence, in accordance with the sensitivity that had previously been derived.

5.1 Application to the IceCube IC40 data sample

The same parameter optimisation and search has been performed with the public data sample[2] from an analysis searching for neutrino pointlike sources [37] of the ICECUBE observatory in its 40-string configuration. These data cover April 2008 to May 2009 and comprise 12877 neutrino candidates. The selection procedure of neutrinos and GRBs is the same as in Sect. 4. With a resolution of 0.7° [38] it leads to 60 GRBs (respectively 12 with measured z) 35 of which are expected to be in coincidence with neutrinos (respectively 4). The different parameters summarising the ANTARES and ICECUBE samples, including the number of coincident events n_{coinc} that would be expected if the neutrino data was completely uncorrelated with the chosen GRBs (i.e., the background-only hypothesis) are given in Table 3.

The ICECUBE GRB sample shows significantly lower statistics, due to the fact that the published data spans only around one year compared to almost six years in the ANTARES sample. In addition, because of the location of the detectors on Earth, 87% of the sky is visible for the ANTARES detector with unequal coverage, whilst the ICECUBE experiment covers the northern sky but at all times. It is also worth noting that, due to the larger instrumented volume of the detector,

---

Table 3 Total live-time of the considered neutrino telescope data sets τ_{tot}, respective number of neutrino candidate events N_{events} and respective median angular resolution $m(\delta)$. Samples of N_{GRB} GRBs are identified (out of which $N_{GRB,z}$ have measured redshifts) for the search of correlations. Assuming totally uncorrelated neutrino data, the mean numbers of coincident events that would be expected within the GRB's search windows n_{coinc} are also given

ν Data sample	τ_{tot} [d]	N_{events}	$m(\delta)$ [°]	δ_{max} [°]	τ_{max} [d]	N_{GRB}	$N_{GRB,z}$	(Uncorrelated) n_{coinc}	$n_{coinc,z}$
ANTARES (07-12)	2154	5516	0.38	0.51–1.59	40	563	150	3.9	0.7
IC40 (08-09)	408	12876	0.70	0.95–2.99	40	60	12	35.0	4.0

Table 4 Mean and median values of the different test statistics used in this analysis as derived in the pseudo experiments of background and in the measurement using the neutrino candidates as selected in the ANTARES data from 2007 to 2012 and ICECUBE data from the IC40-period from April 2008 to May 2009. The number of data events coinciding spatially with the respective GRB samples n_{coinc} are also given. The probabilities $P(>\text{meas})$ and the p-value, $P(\geq\text{meas})$ give the fraction of background-only pseudo experiments that yield test statistics above and at and above the measurement. Being 10 times the logarithm of two definite positive quantities, the ψ type test statistics are usually expressed in dB [28]. Note that since there are no coincidences in the ANTARES data sample, r is not defined

| | ANTARES 07-12 | | | | | ICECUBE IC40 08-09 | | | | | | |
| | All GRBs | | GRBs w/z | | | All GRBs | | | GRBs w/z | | | |
	n_{coinc}	ψ (dB)	n_{coinc}	ψ_z	ψ_{LIV} (dB)	n_{coinc} (dB)	r	ψ (dB)	n_{coinc}	ψ_z	ψ_{LIV} (dB)	(dB)
Bgd mean	4.4	77.4	0.7	11.9	4.5	1.1	35.0	371.3	4.0	56.6	10.4	
Bgd median	4	73.3	0	0	0	35	1.0	371.8	4		56.3	7.9
Measurement	0	0	0	0	0	42	0.4	416.0	8	1.1	93.9	8.8
$P(>\text{meas.})$	98.8%	98.8%	48%	48.6%	48.6%	10.4%	0.4	14.0%	2.1%		6.1%	45.1%
$P(\geq\text{meas.})$	100%	100%	100%	100%	100%	13.5%		14.0%	5.1%		6.1%	45.1%

the ICECUBE data set contains more neutrino candidates than the ANTARES one, while covering a smaller time period in which less GRB alerts were recorded. Both samples therefore explore different statistical regimes. In the end, 42 of the neutrino candidates fall within the search windows, with 8 for the bursts with measured z. This is a slight fluctuation above the expectations from background, with p-values of 13.5% (whole sample) and 5.1% (GRBs with measured redshift), yielding excesses of moderate 1.5σ and 1.9σ significances, respectively. The observation is compatible with no correlation of the ICECUBE data with the chosen GRB sample. Moreover, the timing profiles show no indication for any preferred time delay. The measured and expected values as well as the corresponding significance of the different test statistics for the two studied samples, are summarised in Table 4.

6 Conclusion

A powerful method has been presented to identify a neutrino signal associated with GRBs if it is shifted in time with respect to the photon signal. The signal is distinguished from randomly distributed data as a cumulative effect in stacked timing profiles of spatially coincident neutrinos in the data from the ANTARES and ICECUBE neutrino telescopes.

Estimating the behaviour of the search for a large number of simulated measurements using randomised sky maps of the neutrino events, and comparing these with the actual neutrino telescope data, significances of the observations were derived. Using data from the ANTARES neutrino telescope between the years 2007 and 2012, a deficit of spatially coincident neutrinos with the selected gamma-ray-burst catalogue was reported, with 98.8% of the randomised data leading to more coincidences between the neutrino data and the GRBs. The application of the method to the public ICECUBE data in its 40 line configuration gives results compatible with the expectation from background.

The presented approach could have identified an intrinsically time-shifted signal even if only of the order of one in a hundred GRBs would have given rise to a single associated neutrino in the ANTARES data. This is above the detectable neutrino signal predicted by the NeuCosmA model [39] that is on average only of the order of $\sim 2 \times 10^{-4}$ in the ANTARES detector, and only the strongest individual burst yields a neutrino detection rate exceeding 0.01 [12].

In conclusion, novel analysis techniques have been developed that increase the sensitivity of existing neutrino searches from GRBs to models of delayed neutrino emission and

Lorentz Invariance Violation. They allow extending the search for neutrinos from GRBs with time displacements of up to 40 days. It confirms the absence of a significant neutrino signal being associated with GRBs that has so far been measured in the simultaneous time windows.

References

1. E. Waxman, Phys. Rev. Lett. **75**, 386 (1995)
2. E. Waxman, J. Bahcall, Phys. Rev. Lett. **78**, 2292 (1997)
3. E. Waxman, Astrophys. J. Suppl. **127**, 519 (2000)
4. S. Fukuda et al., Astrophys. J. **578**(1), 317 (2002)
5. A. Achterberg et al., Astrophys. J. **674**(1), 357 (2008)
6. A.V. Avrorin et al., Astron. Lett. **37**(10), 692 (2011)
7. D. Besson et al., Astropart. Phys. **26**(6), 367 (2007)
8. A.G. Vieregg et al., Astrophys. J. **736**(1), 50 (2011)
9. R. Abbasi et al., Astrophys. J. **710**, 346 (2010)
10. R. Abbasi, Nature **484**, 351 (2012)
11. S. Adrián-Martínez, JCAP **03**, 006 (2013)
12. S. Adrián-Martínez, A&A **559**, A9 (2013)
13. D. Guetta, Astropart. Phys. **20**, 429 (2004)
14. J. Casey for the IceCube Collaboration, in *Proceedings of the 33rd ICRC*, ed. by IUPAP (2013)
15. S. Razzaque, Phys. Rev. D **68**(8), 083001 (2003)
16. E. Waxman, J.N. Bahcall, Astrophys. J. **541**, 707 (2000)
17. G. Amelino-Camelia, L. Smolin, Phys. Rev. D **80**(8), 084017 (2009)
18. U. Jacob, T. Piran, Nat. Phys. **3**, 87 (2007)
19. G. Amelino-Camelia et al., Astrophys. J. **806**(2), 269 (2015)
20. M. Ageron, Nucl. Instrum. Methods A **656**, 11 (2011)
21. S. Adrian-Martinez et al. (ANTARES and IceCube Collaborations), Astrophys. J. **823**(1), 65 (2016)
22. S. Adrian-Martinez, Astrophys. J. **786**, L5 (2014)
23. N. Gehrels, Astrophys. J. **611**, 1005 (2004)
24. W.B. Atwood, Astrophys. J. **697**, 1071 (2009)
25. C. Meegan, Astrophys. J. **702**, 791 (2009)
26. J.A. Aguilar, for the IceCube Collaboration, in *Proceedings of the 33rd ICRC*, ed. by IUPAP (2013)
27. N. van Eijndhoven, Astropart. Phys. **28**, 540 (2008)
28. D. Bose, Astropart. Phys. **50**, 57 (2013)
29. K.A. Olive et al. (Particle Data Group), Review of particle physics. Chin. Phys. C **38**, 090001 (2014)
30. D.E. Alexandreas, Nucl. Instrum. Methods A **328**, 570 (1993)
31. S. Adrian-Martinez et al. Astrophys. J. **760**, 53 (2012)
32. J. Granot, D. Guetta, Phys. Rev. Lett. **90**(19), 191102 (2003)
33. K. Murase, Phys. Rev. D **76**(12), 123001 (2007)
34. S. Razzaque, Phys. Rev. D **88**(10), 103003 (2013)
35. V. Vasileiou, Phys. Rev. D **87**(12), 122001 (2013)
36. M.G. Aartsen, Astrophys. J. **779**, 132 (2013)
37. R. Abbasi, Phys. Rev. D **84**, 082001 (2011)
38. A. Karle for the IceCube Collaboration, in *Proceedings of the 31rst ICRC*, ed. by M. Giller, J. Szabelski (2009)
39. S. Hümmer, M. Rüger, F. Spanier, W. Winter, Astrophys. J. **721**, 630 (2010)